# Carbon Incorporation in Pd(111) by Adsorption and Dehydrogenation of Ethene

**Harald Gabasch,[†,‡] Konrad Hayek,[†] Bernhard Klötzer,*[,†] Axel Knop-Gericke,[‡] and Robert Schlögl[‡]**

*Institut für Physikalische Chemie, Universität Innsbruck, A-6020 Innsbruck, Austria, and Abteilung Anorganische Chemie, Fritz-Haber-Institut der Max-Planck-Gesellschaft, Faradayweg 4-6, D-14195 Berlin, Germany*

*Received: November 22, 2005; In Final Form: January 26, 2006*

The decomposition of ethene on the Pd(111) surface was studied at effective pressures in the $10^{-8}$ to $10^{-7}$ mbar range and at sample temperatures between 300 and 700 K, using an effusive capillary array beam doser for directional adsorption, LEED, AES, temperature programmed reaction, and TDS. In the temperature range of 350−440 K increasingly stronger dehydrogenation of the ethene molecule is observed. Whereas at 350 K an ethylidyne adlayer is still present after adsorption, already at temperatures around 440 K complete coverage of the surface by carbon is attained, while the bulk still retains the properties of pure Pd. Beyond 440 K a steady-state surface C coverage is established, which decreases with temperature and is determined by detailed balancing between the ethene gas-phase adsorption rate and the migration rate of carbon into the Pd bulk. This process gives rise to the formation of a "partially carbon-covered $Pd_xC_y$ surface". Above 540 K the surface−bulk diffusion of adsorbed carbon becomes fast, and in the UHV experiment the ethene adsorption rate becomes limited by the ethene gas-phase supply. The carbon bulk migration rate and the steady-state carbon surface coverage were determined as a function of the sample temperature and the ethene flux. An activation energy of 107 kJ $mol^{-1}$ for the process of C diffusion from surface adsorption sites into the subsurface region was derived in the temperature range of 400−650 K by modeling the C surface coverage as a function of temperature on the basis of steady-state reaction kinetics, assuming a first-order process for C surface−subsurface diffusion and a second-order process for C(ads) formation by dissociative $C_2H_4$ adsorption.

## 1. Introduction

Palladium-containing supported catalysts are important in hydrocarbon combustion[1−3] and are also frequently used in the selective oxidation of small hydrocarbons, e.g., of ethene, to acetaldehyde or acetic acid,[4−7] and of ethene plus acetic acid to vinyl acetate.[8−10] For total oxidation processes such as methane combustion, PdO has been proposed as the most active phase.[11−13] In contrast, selective partial oxidation requires a more reduced state of Pd as the active phase. It seems that in the case of selective oxidation of ethene and of vinyl acetate synthesis a near-surface modification of Pd metal with carbon is most effective.[14,15] More knowledge about the decomposition of unsaturated or functionalized hydrocarbons on Pd surfaces, leading to adsorbed or dissolved carbon, is therefore required.

The present paper is dedicated to the interaction of ethene with the Pd(111) surface at temperatures close to "actual" reaction conditions, e.g., of vinyl acetate synthesis (around 450 K). The adsorption of ethene on Pd(111) at low temperature was investigated previously, e.g., by infrared spectroscopy,[16] electron energy loss spectroscopy,[17] and high-resolution XPS.[18] It is well established that below 200 K ethene is molecularly adsorbed as a di-$\sigma$- or $\pi$-bonded species, while at about 300 K it dissociates forming ethylidyne on the surface.[17−19] In this temperature range the C−C bond is not dissociated, and the interaction of the molecule with the metal is limited to the surface. At temperatures beyond 400 K ethene decomposes more or less completely. CH species and CCH species have been observed in this temperature range.[20,21]

While interactions of $C_2H_4$ with Pd single-crystal surfaces at room temperature and below are well described, the detailed mechanism of the decomposition at higher temperature and the fate of the formed carbon-containing surface species and their relevance for catalysis are still under scrutiny. From the work of Ziemecki et al.[22] it is known that Pd undergoes a phase transformation if the metal is exposed to carbon-containing gases such as ethyne or ethene at atmospheric pressure above 423 K. The new phase is manifested by an expansion of the Pd unit cell and decomposes above 873 K in inert atmosphere. By analyzing the depth profiles of carbon these authors detected a diffusion front of carbon moving as a function of ethylene exposure. The solubility of carbon in palladium was studied by Siller et al.[23] over a wide temperature range. A recent study of the Pd/C system by Paál et al.,[24] using photoelectron spectroscopy (XPS und UPS), confirmed changes of the valence state of Pd black upon ethene exposure, indicating appreciable Pd−C interactions.

A study with high-resolution electron energy loss spectroscopy (HREELS) by Jungwirthova and Kesmodel[21] suggests that, up to 350 K, ethylidyne is the predominant surface species observed after both ethene and ethyne adsorption. Above 350 K the situation is less clear; the existence of a partially dehydrogenated adlayer was observed up to 400 K, and depending on the adsorbate (ethene or ethyne) CH or CCH species were proposed.[20,21]

Detailed recent investigations by Bowker and co-workers[25,26] of the decomposition of acetic acid and of the adsorption of

* Corresponding author. Phone: +43 512 507 5071. Fax: +43 512 507 2925. E-mail: bernhard.kloetzer@uibk.ac.at.
[†] Universität Innsbruck.
[‡] Fritz-Haber-Institut der Max-Planck-Gesellschaft.

10.1021/jp056765g CCC: $33.50 
Published on Web 02/22/2006

ethene on Pd (110) under UHV conditions revealed that above 450 K the sticking rates of acetic acid and ethene reach a steady state and that the surface is not poisoned by the buildup of carbon. They concluded that the carbon remains in the selvedge, i.e., in the immediate subsurface region, and can therefore be removed by $O_2$ clean-off.

Several approaches have been undertaken to determine the influence of *surface* carbon species on the reactivity of Pd surfaces. The formation of carbonaceous residues affects both the decomposition and oxidation of carbon-containing molecules. Shaikhutdinov et al.[27] attempted to rationalize the effects of carbon deposits on small palladium particles on the adsorption of CO and ethene, while Bertarione et al.[28] observed that carbon contamination may influence the reaction pathway of methanol decomposition by blocking edge and defect sites on the particle surface. More detailed information about the composition and further reaction of $CH_x$ overlayers was obtained in a high-pressure study by Morkel et al.,[29] with help of vibrational sum frequency generation (SFG) and X-ray photoelectron spectroscopy (XPS). Borasio et al.[30] reported that surface carbon species promoted formaldehyde formation from methanol at 300 K by limiting formaldehyde decomposition to CO.

Some of the present authors observed recently that polycrystalline palladium foil exhibits its highest selectivity for partial oxidation of ethene to acetic acid at a temperature of about 423 K, e.g., in the temperature range where, according to the present work, mainly near-surface carbon is formed. They could also show that a high-temperature pretreatment of the Pd surface with ethene, resulting in pronounced carbon accumulation, markedly enhances the selectivity toward partial oxidation.[15]

To rationalize the reported catalytic effects, it is of primary importance to elucidate the adsorption and decomposition of ethene and the bulk migration of the resulting carbon deposits, which is the focus of this work on the Pd(111) single-crystal surface between 400 and 700 K.

## 2. Experimental Section

The UHV chamber for kinetic measurements was equipped with low-energy electron diffraction (LEED), Auger electron spectroscopy (AES), an effusive beam doser based on a capillary array for directional adsorption experiments (Galileo Optics, setup similar to that reported in ref 31), and a differentially pumped quadrupole mass spectrometer (QMS) for line-of-sight detection of molecules desorbing from the central part (a 3 mm ø spot) of the Pd(111) face. Calibration of beam fluxes was achieved by measurement of the pressure decrease in a differentially pumped gas-dosing system by means of an MKS Baratron absolute pressure transducer. A second QMS monitoring the pressure changes in the main chamber was used for King and Wells sticking measurements.[32] In the given geometry 90% of the gas effusing from the doser hit the sample, as determined by comparison of the observed initial sticking probability of $O_2$ with data from supersonic beam experiments.[33] Throughout this work, coverages and beam fluxes refer to 1 ML (monolayer) as a 1:1 ratio of carbon atoms to $1.53 \times 10^{15}$ Pd surface atoms $cm^{-2}$ in the (111) bulk-terminated geometry.

The Pd(111) sample (12 mm ø, 3 mm thick) was oriented within 0.2° of the bulk (111) plane and cleaned by flashing to 1250 K, sputtering with 700 eV $Ar^+$, flashing to 1200 K, exposure to $5 \times 10^{-7}$ mbar of oxygen during cooling from 1200 to 600 K, and final annealing to 1200 K. Cleanliness was checked by AES and flash desorption of adsorbed oxygen and/or CO. Temperature programmed desorption (TPD) and temperature programmed reaction (TPR) experiments were carried out with a linear heating ramp of 10 K $s^{-1}$.

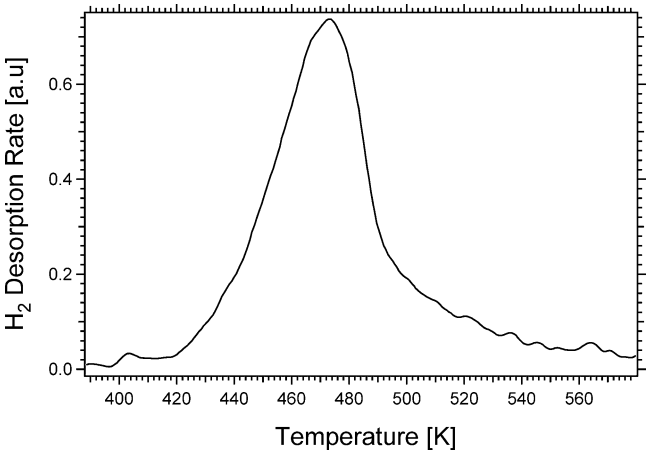


**Figure 1.** TPR spectrum of $H_2$ formed by decomposition of a complete 0.33 ML ethylidyne adlayer, prepared by exposure to 43 ML of $C_2H_4$ at 350 K. Heating rate: 10 K $s^{-1}$.

## 3. Results and Discussion

**3.1. Ethene Decomposition at $T \leq 440$ K.** To study the decomposition of ethylidyne on the Pd(111) surface, we recorded TPD spectra of reactive $H_2$ desorption as a function of temperature in front of the differentially pumped line-of-sight mass spectrometer, without being disturbed by hydrogen background effects.

The Pd (111) surface was saturated by exposure to an ethene beam (flux, 0.048 ML $s^{-1}$) at 350 K for 15 min, resulting in the previously reported $(\sqrt{3} \times \sqrt{3})R30°$ LEED pattern ascribed to a 0.33 ML ethylidyne coverage.[18] The main surface species after adsorption at 350 K is ethylidyne, as was also concluded from HREELS data.[21] Figure 1 shows the reactive $H_2$ desorption spectrum arising from the decomposition of this adlayer to carbon and hydrogen. We note that our experiment yields only one single $H_2$ peak with a maximum at 473 K, appearing at a somewhat higher temperature as reported previously.[34] This can be explained by the different preparation conditions. In ref 34 the sample was exposed to $C_2H_4$ at 175 K, i.e., in a temperature range of mainly molecular adsorption of ethene. In that case, the main part of ethene desorbs again molecularly during the TPD experiment and presumably no full ethylidyne adlayer is formed, leaving a part of the surface free of carbon-containing adsorbates.[18,20] In our experiment the surface was deliberately covered with a full $C_2H_3$ layer forming a $(\sqrt{3} \times \sqrt{3})R30°$ LEED pattern, which requires ethene dosing at room temperature and beyond.[18,21] We can assume that for the dehydrogenation of $C_2H_3$ the absence of neighboring free adsorption sites is detrimental, which may explain the observed shift of the peak maximum to higher temperatures. Furthermore, the shape of the desorption trace suggests fast and complete decomposition of the $C_2H_3$ species; features appearing at higher temperature than the main peak, indicating stepwise decomposition with increasing temperature, are missing. The temperature of the peak maximum of 473 K indicates that the rate-determining step for $H_2$ evolution is definitely the *decomposition* and not $H_2$ desorption, which exhibits a peak maximum below 400 K.[35]

To study isothermal ethene adsorption kinetics, particularly in the temperature range relevant for ethylidyne decomposition, the sample was exposed to a beam flux of 0.048 ML $s^{-1}$ ethene at a constant temperature chosen between 373 and 473 K, and the hydrogen $m/z = 2$ and the ethene $m/z = 27$ intensities were

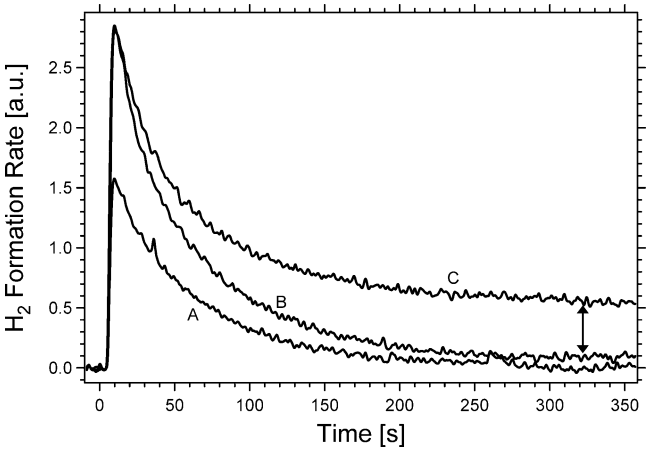


**Figure 2.** $H_2$ formation rate measured during $C_2H_4$ exposure (beam flux 0.048 ML $s^{-1}$) at different sample temperatures: 413 K (A), 433 K (B), 453 K (C).

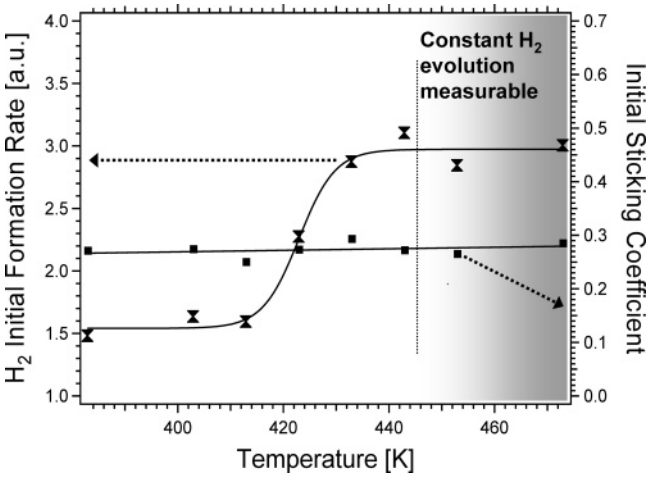


**Figure 3.** Initial $H_2$ formation rate (bipyramids) and initial sticking coefficient of $C_2H_4$ (squares) as a function of temperature. Temperatures at which constant $H_2$ formation was observed are above 446 K (marked by the bar/shaded area).

monitored simultaneously. Figure 2 shows three characteristic $H_2$ formation traces obtained during exposure at 413 K (A), 433 K (B), and 453 K (C). Between 413 and 433 K both the initial $H_2$ formation rate and the integral amount of $H_2$ increase, obviously because of faster and more complete dehydrogenation of adsorbing $C_2H_4$. Since in case B the rate approaches zero after some time, we may assume that the surface saturates with a more strongly dehydrogenated carbonaceous adlayer than in case A. Surprisingly, at 453 K and beyond (trace C), an additional *steady-rate* contribution assigned to continuous ethene dissociation is superimposed onto the fast process of surface-limited decomposition of trace B (arrow). This continuous process was observed to occur, at a given temperature, with a constant rate over long periods of time (>60 min was tested), and this constant rate was found to increase with sample temperature. The fact that both the $H_2$ evolution and the adsorption rate remain constant while the crystal is hit by the beam (Figure 5), implies that also free adsorption sites for ethene decomposition must be formed at a constant rate. This can be only understood by assuming a steady loss of carbon into the sample bulk at the respective temperatures above 440 K.

In Figure 3 the *initial* hydrogen formation rate and the corresponding *initial* ethene sticking coefficient are plotted as a function of sample temperature over a wider temperature range (350−475 K). While the initial ethene sticking probability

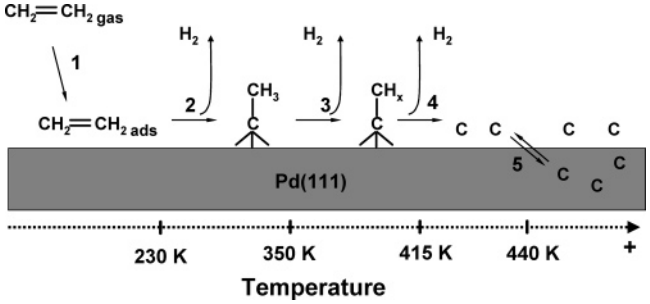


**Figure 4.** Mechanistic scheme of ethene dehydrogenation on the Pd(111) surface as a function of temperature.

(determined according to King and Wells[32]) remains almost constant at about 0.28 and is virtually not affected by the temperature, the corresponding initial hydrogen formation rate increases steeply between 425 and 435 K and then approaches an upper limit. Furthermore, this higher *initial* $H_2$ formation rate is not influenced by the onset of carbon incorporation at $T > 440$ K which, on the other hand, is accompanied by a constant contribution to the *integral* $H_2$ evolution (shaded area) over the whole exposure time. This can also be rationalized by comparing traces B and C in Figure 2: they exhibit the same initial hydrogen formation rate, but the integral of trace C over time yields considerably more $H_2$.

Between 380 and 410 K both the initial hydrogen formation rate (Figure 3) and the integral amount of $H_2$ produced during ethene adsorption are limited to a constant lower value (Figure 2, integral of curve A). This indicates that the adsorbate stoichiometry does not strongly change in this temperature range. While at 350 K a complete ethylidyne adlayer can be assumed,[21] less is known about the adsorbate stoichiometry in the temperature range of 350−410 K. In ref 21 the particularly stable CCH moiety was observed as the main product of ethylidyne decomposition at around 400 K. We may assume partial dehydrogenation of ethene to CCH at $T < 410$ K and complete dehydrogenation of ethene via intermediate CCH to carbon at $T > 440$ K, whereby both assumptions are supported by HREELS.[21] In this case the rate of $H_2$ formation as well as the integral $H_2$ formed should increase approximately by a ratio of approximately 4:3 when changing the temperature, e.g., from 400 to 450 K. However, Figure 3 rather suggests a ratio of 2:1, corresponding to a "mean" $C_2H_2$ or CH stoichiometry of the adlayer formed at 400 K. Since the main spectral features of ethylidyne do not instantaneously vanish but become progressively weaker above 350 K,[21] rather a $CCH_3$/CCH mixed adlayer appears to be present between 350 and 410 K, which would provide a tentative explanation of the observed 2:1 ratio.

Merging our results with the existing knowledge from literature allows us to derive a schematic model of ethene adsorption on Pd(111) as a function of sample temperature (Figure 4), similar to the model proposed by Bowker et al. on Pd(110).[26]

Three of the five main reaction steps in Figure 4 cause $H_2$ evolution: ethylidyne formation from adsorbed ethene (step 2), the subsequent decomposition of the ethylidyne species toward CCH (step 3), and the dehydrogenation of CCH (step 4). Step 5 represents the permeation of C atoms through the surface occurring without $H_2$ release. From the results of Figure 3 we conclude that the initial ethene sticking coefficient and the ethene adsorption rate at free adsorption sites are not temperature-dependent and step 1 is not activated. Hence, the ethene adsorption rate from the gas phase depends only on the effective pressure (flux) and on the number density of available adsorption

sites. Steps 2−5 appear to be activated in a progressive order, since they sequentially come into action with increasing temperature. If we assume that the activation barrier of step 5 is clearly the highest, we must anticipate that the highest initial $H_2$ formation rate and the largest integral $H_2$ formation will precede the process of continuous subsurface carbon loss, because complete dehydrogenation of ethene and its fragments to a surface carbon overlayer must take place at a higher rate prior to the slower subsurface migration. This suggests that at ∼440 K the metal bulk is little influenced by carbon and mainly pure Pd covered by a basically complete C adlayer is present. Experimentally, both Figure 2B and Figure 3 confirm that the fastest and $H_2$-richest decomposition process occurs at $T \geq 440$ K, yielding such a carbon adlayer on the surface *before* a steady-state reaction rate for C subsurface migration is established. Beyond this temperature limit the *initial* $H_2$ formation rate should be independent of temperature since all impinging molecules loose all their hydrogen atoms quickly (confirmed again by Figures 2 and 3). In contrast, the constant $H_2$ formation rate caused by subsurface loss of C, which is proportional to the re-formation rate of new ethene adsorption sites, should further increase with $T$, as more adsorption sites will become available per time the faster adsorbed carbon goes subsurface. The system becomes more complex, now consisting of "partially carbon-covered $Pd_xC_y$" near the surface (Figure 4).

**3.2. Subsurface Migration of Carbon.** The nature of the carbon-containing dehydrogenated surface adlayer present at 440 K and beyond deserves a more detailed discussion, since its composition is important for the subsequent process of carbon dissolution. In an EELS study Nishijima et al.[36] observed complete dehydrogenation and decomposition of ethinyl species CCH toward 2 C(ad) at $T = 520$ K. On the basis of their spectra they exclude the existence of $C_n$ species with $n > 1$ or a graphitic adlayer at $T \geq 520$ K. Therefore, it is safe to assume that the rate-determining step of C subsurface migration is the C atom diffusion from surface to subsurface sites at least in the temperature region above 520 K. Unfortunately, no spectra are available from ref 36 in the temperature region from 440 to 520 K. The 400 K spectra are dominated by the presence of the ethinyl species, but the exact temperature of ethinyl decomposition toward C(ad) cannot be deduced. Thus, a *steady* partial coverage of the surface with CCH cannot be excluded for the region between 440 and 520 K. Nevertheless, it appears unlikely that the microkinetic mechanism of C subsurface migration changes completely between 440 and 520 K. It appears more likely that between 440 and 520 K the CCH species is at a higher steady *intermediate* coverage toward C(ad) formation. But since CCH is essentially an intermediate approaching zero concentration at >520 K, its decomposition must be less activated than the subsequent C subsurface migration process, which is rate-determining at $T > 520$ K. Further support of C adatom diffusion from the surface to the subsurface region as the rate-limiting microkinetic process is provided by the work of Bowker et al.,[25] who investigated the adsorption and decomposition of acetic acid on Pd(110). From TPD and molecular beam experiments these authors concluded that adsorbed acetic acid starts to decompose (decarboxylate) to $CO_2$ and C on the surface above 320 K. If an adlayer of acetic acid is decomposed thermally, the $CO_2$ and $H_2$ evolution is complete at 450 K, indicating both complete decarboxylation and C1 dehydrogenation. C(ad) is therefore formed already at temperatures well below 450 K, but the steady-state decomposition of acetate indicating subsurface migration of surface carbon atoms becomes fast at 473 K, quite close to the onset of carbon migration observed in the present work. Acetic acid decomposition clearly proceeds via a C1 intermediate toward C(ad). Therefore, we conclude that in both cases (acetic acid and ethene) the C subsurface migration process proceeds via a C(ad) atom overlayer and that the subsurface migration of the latter is rate-determining at $T > 440$ K.

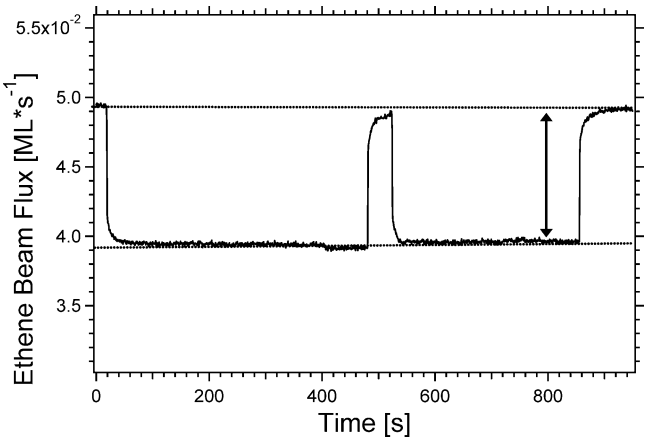


**Figure 5.** Flux-calibrated ethene $m/z = 27$ intensity change obtained by turning the Pd(111) surface in to and out of the ethene molecular beam at 523 K (beam flux: 0.048 ML $s^{-1}$).

To obtain more information about carbon migration through the surface, ethene adsorption experiments were carried out at different sample temperatures above 440 K. The clean Pd (111) surface was exposed to a molecular beam of ethene (calibrated beam flux, 0.048 ML $s^{-1}$). The scenario discussed in section 3.1 is clearly suggested by Figure 5: upon turning the sample into the ethene beam at $T = 523$ K, a steady-rate adsorption process (and constant $H_2$ production, not shown) caused by continuous ethene decomposition and C subsurface loss is established, in close analogy to Pd(110).[26] Since absolute beam fluxes were low and the Pd bulk apparently acts as an almost infinite sink for carbon, the steady-state rates were constant at least for several hours. Recent STM measurements of the lateral diffusion of carbon subsurface impurities residing in the first interlayer of the Pd bulk were interpreted in terms of a rather low diffusional barrier for C atom in-bulk diffusion,[37] as compared to the C surface-to-bulk permeation barrier. According to ref 37 it is therefore not possible to accumulate much C in the near-surface region by exposure to a carbon source, at least under UHV conditions. This supports our experimental finding that the surface-to-bulk migration of C atoms is essentially irreversible under our experimental conditions. Obviously, the subsurface C atoms are moving rapidly into deeper layers and reside inside the bulk in a highly diluted state.

The quantitative contribution of the "constant net adsorption rate" at 523 K is indicated in Figure 5 by two dashed lines. The level of the upper line is proportional to the ethene flux into the chamber while the molecular beam enters without hitting the crystal, and the lower line indicates the residual flux while the crystal is hit by the gas. The fraction of adsorbed relative to unreacted ethene, i.e., the constant net adsorption rate, can be directly derived. It is related to the net adsorption rate of carbon atoms generated via complete ethene dehydrogenation by a factor of 2, i.e., $2R_{ads}(C_2H_4) = R_{ads}(C)$. Since sticking and adsorption rates are constant over time, the C bulk *absorption* rate must equal the C net adsorption rate: $R_{sub}(C) = R_{ads}(C)$.

The constant $H_2$ production was also measured, but the corresponding data could not be calibrated because of $H_2$

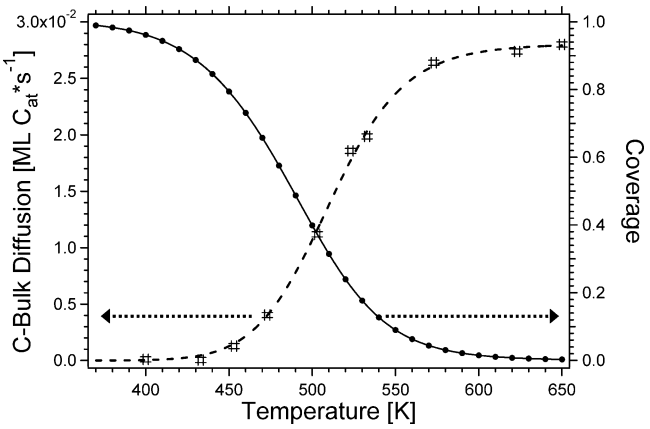


**Figure 6.** Experimental and model-calculated carbon bulk diffusion rate (# symbols and dashed line, respectively) and surface carbon coverage (solid line/full circles) as a function of temperature. The fit of the calculated rate to the experimental values is based on $\nu_C = 3.9 \times 10^9$ s$^{-1}$, $E_{sub,C} = 107$ kJ mol$^{-1}$, $S_{ethene}{}^0 = 0.28$, and an ethene flux of 0.048 ML s$^{-1}$.

background effects, unquantified absorption effects of hydrogen in the bulk and fragmentation of ethene to $H_2$ by the QMS ion source.

Since the *initial* ethene sticking and adsorption rate are virtually temperature-independent (Figure 3), while subsurface C migration is certainly activated and should become much faster with increasing temperature, we anticipated a pronounced temperature dependence of the number density of free adsorption sites and the carbon coverage, respectively, and thus of the net adsorption rate. Figure 6 compiles a set of steady-rate experiments at different temperatures: the C adsorption/bulk migration rate increases exponentially in the range between 440 and 520 K and approaches an upper limiting value at around 600 K, which already comes close to the maximum gas-phase supply of 0.048 ML s$^{-1}$ ethene, corresponding to 0.096 ML s$^{-1}$ carbon. This strongly suggests that the steady-state carbon coverage *on* the surface changes from full coverage at around 440 K to low coverage at around 600 K.

To quantify our experimental results, a simplified steady-state kinetic model for ethene dissociative adsorption to adsorbed carbon, followed by subsurface migration of C, was tested in order to estimate the temperature dependence of the rate of C adsorption/absorption and of the steady-state surface C coverage. The following assumptions were made with respect to the change of surface C coverage $\Theta_C$:

$$\frac{d\,\Theta_C}{dt}(\text{ads}) = 2(\text{flux}_{C_2H_4})(s_{C_2H_4}{}^0)(1 - \Theta_C)^2 \qquad (1)$$

The first rate equation accounts for C supply from the gas phase and implies that dissociative adsorption of ethene to form two C atoms requires at least two adjacent free sites. Of course this assumption ignores all the intermediates of this complex process, ethylidyne and the more strongly dehydrogenated molecular surface species. This expression is a rather crude but deliberate simplification, but it may be justified: The first step of *dissociative* ethene adsorption toward ethylidyne occurs with a high rate already at temperatures well below 273 K and is irreversible (ethylidyne does not react back to ethene even in the presence of H atoms). Irrespective of mechanistic details, two C atoms are eventually formed at a high rate, requiring at least two adjacent adsorption sites, e.g., if the C−C bond of a CCH or $CCH_3$ moiety is broken.

Equation 2 represents the irreversible and thermally activated loss of surface-adsorbed C by subsurface migration:

$$\frac{d\,\Theta_C}{dt}(\text{sub}) = \Theta_C \nu_C \exp(-E_{C,sub}/RT) \qquad (2)$$

We follow the argument of Yudanov et al.,[38] who showed by DFT that this process starts with a C atom in a surface fcc binding site, proceeds via a "through-surface" transition state of well-defined geometry and activation energy, and leads to the formation of a subsurface C atom in an octahedral interstitial site, which can then travel easily into deeper layers. We assume that the surface-to-bulk diffusion barrier is essentially higher than the bulk-related barrier for diffusion between interstitial sites; thus, a subsurface carbon atom can travel easily over a somewhat longer distance, and a lack of free subsurface sites should not significantly block subsurface diffusion.

In the beginning of ethene exposure of the clean sample, the C coverage is zero and the C adsorption rate exceeds the carbon bulk loss. After some time a steady-state situation is established where the adsorption rate and the bulk migration rate are evenly balanced, as can be directly seen from experiment C in Figure 2. This means that the rates in eqs 1 and 2 become equal:

$$\frac{d\,\Theta_C}{dt}(\text{ads}) - \frac{d\,\Theta_C}{dt}(\text{sub}) = 0$$

By equating (1) and (2) a second-order equation with respect to $\Theta_C$ is obtained. Its solution provides an explicit expression for the carbon coverage as a function of temperature, subsurface diffusion preexponential, and activation energy, at a given ethene beam flux. By entering this expression into eqs 1 or 2 the ethene adsorption rate and the C bulk migration rate, respectively, can be calculated. The result is plotted in Figure 6 in direct comparison to the experimental data for the steady-state C bulk diffusion rate (equal to the steady-state ethene adsorption rate $\times$ 2). The already known values for the beam flux and the initial ethene sticking were entered into the fitting procedure, and only the subsurface diffusion preexponential and activation barrier were chosen as free parameters in the least-squares refinement. The model calculation results in a preexponential $\nu_C = 3.9 \times 10^9$ s$^{-1}$ and an activation barrier $E_{C,sub} = 107$ kJ mol$^{-1}$. The fitting procedure was also tested for the case of first-order adsorption kinetics of ethene, using $(1 - \Theta_C)$ instead of $(1 - \Theta_C)^2$ in eq 1. The values derived for the preexponential and activation energy were found to be very similar as compared to those of the second-order fit, i.e., $\nu_C = 3.9 \times 10^9$ s$^{-1}$ and $E_{C,sub} = 108$ kJ/mol, respectively. The convergence of the fit was slightly better for second-order adsorption kinetics (shown in Figure 6, dashed line). Essentially, it does not matter very much for the numerical value of the activation barrier which effective space requirement of dissociative ethene adsorption is chosen and whether more or less intermediate CCH ethinyl species cover the surface, since they as well decompose toward two C adatoms, which again requires most likely two adjacent adsorption sites. The main result is that at 440 K the surface is covered by a complete layer of single C(ad) atoms and in part by CCH species, thus blocking ethene adsorption completely, and that at 650 K the steady C(ad) surface coverage approaches zero. Consequently both the number of single free metal sites and the number of pair sites increases from zero to the maximum value on the adsorbate-free surface in the same temperature range. For this reason the numerical value of the activation energy does hardly depend on the order of the adsorption kinetics with respect to the concentration of free adsorption sites.

Generally, the effective space requirement of dissociative ethene adsorption is not known.

The activation barrier of 107 kJ/mol derived by modeling our experimental data deserves a closer look at the literature. Recent theoretical work of Yudanov et al.,[38] who studied the incorporation of atomic H, C, O, and N into Pd nanoparticles using DFT, predicts an activation barrier for carbon atoms migrating from a surface fcc site to a subsurface octahedral site of 0.62 or 0.81 eV, i.e., 60 or 78 kJ/mol (depending on the particular density approximation), proceeding via a highly ordered, sterically well-defined and complex single transition state of particularly high symmetry. Interestingly, the barrier calculated for H atoms is even somewhat higher, at around 0.62/0.91 eV, i.e., 60/88 kJ/mol, although experimentally H dissolution in Pd occurs at lower temperatures than C dissolution. In both cases the energetically most favorable, but entropically disfavored, transition state is addressed. We may speculate about a certain bandwidth of energetically less, but statistically more favorable states, due to the rather large "supramolecular" arrangement of a larger number of atoms in the transition state(s). A strongly negative contribution of activation entropy can as well increase the activation energy and lower the preexponential. We note that the value of our exponential is in a range which is usually accepted for diffusion processes *across* surfaces[39] and that the activation barrier does not strongly exceed those calculated in ref 38. Beyond this argument from transition state theory, the barrier may be considerably lower for nanoparticles, anyway, since elastic relaxation of small particles is expected to be energetically less demanding than that of an infinite metal bulk. This effect has already been reported for hydrogen subsurface and bulk diffusion.[40]

A DFT study by Pallassana et al., focusing on the mechanistic pathway of ethylidyne formation from di-$\sigma$-bonded ethylene, revealed that the activation barrier of intermediate vinyl formation (the rate-determining step) can be as high as 151 kJ/mol.[41] This process takes place already at 300 K with a high rate, in contrast to C subsurface migration which becomes fast at $T >$ 440 K. With respect to this work it appears even more reasonable that the C bulk diffusion barrier is at least as high as 107 kJ mol$^{-1}$. From the experimental viewpoint it is clear that the *rate* of C subsurface migration is the smallest at any temperature, as compared to all other surface processes starting with molecular ethene. At the moment it remains an open issue whether these obvious discrepancies can be explained on the basis of statistical transition state theory.

## 4. Summary and Conclusions

Ethene decomposition on Pd(111) in the temperature range between 440 and 600 K and at effective pressures in the $10^{-8}$ to $10^{-7}$ mbar range is governed by diffusion of carbon from a surface adlayer through the close-packed Pd(111) surface into the Pd bulk, resulting in a "carbon-covered $Pd_xC_y$" surface. Below 440 K only the surface is carbon-covered, but the bulk remains pure Pd. The carbon surface coverage and the migration rate of carbon into the Pd bulk were determined as a function of sample temperature. For the microkinetic step of C atom surface−subsurface diffusion an activation energy of 107 kJ mol$^{-1}$ was derived from a steady-state adsorption−diffusion model based on the assumptions of second-order dissociative ethene adsorption on free surface sites and a first-order process for the transition of a C atom from a surface site to the adjacent subsurface site.

**Acknowledgment.** H.G. acknowledges the German Max Planck Society for providing a research grant.

## References and Notes

(1) Lee, J. H.; Trimm, D. L. *Fuel Process. Technol.* **1995**, *42*, 339.
(2) Kolaczowski, S. T. *Trans. Inst. Chem. Eng.* **1995**, *73*, 168.
(3) Heck, R. M.; Farrauto, R. J.; *Catalytic Air Pollution Control: Commercial Technology*; Wiley: NewYork, 2002.
(4) Xie, J.; Zhang, Q.; Chuang, K. T. *Catal. Lett.* **2004**, *93*, 181.
(5) Sano, K.; Uchida, H.; Wakabayashi, S. *Catal. Surv. Jpn.* **1999**, *3*, 55.
(6) Seoane, J. L.; Boutry, P.; Montarnal, R. *J. Catal.* **1980**, *63*, 191.
(7) Evnin, A. B.; Rabo, J. A.; Kasai, P. H. *J. Catal.* **1973**, *30*, 109.
(8) Stacchiola, D.; Calaza, F.; Burkholder, L.; Tysoe, W. T. *J. Am. Chem. Soc.* **2004**, *126*, 15384.
(9) Han, Y.-F.; Kumar, D.; Sivadinarayana, C.; Clearfield, A.; Goodman, D. W. *Catal. Lett.* **2004**, *94*, 131.
(10) Han, Y.-F.; Kumar, D.; Sivadinarayana, C.; Goodman, D. W. *J. Catal.* **2004**, *224*, 60.
(11) Oh, S.; Mitchell, P. *J. Catal.* **1991**, *132*, 187.
(12) Salomonsson, P.; Johansson, S.; Kasemo, B. *Catal. Lett.* **1995**, *33*, 1.
(13) McCarty, J. G. *Catal. Today* **1995**, *26*, 283.
(14) Bowker, M.; Morgan, C. *Catal. Lett.* **2004**, *98*, 67.
(15) Unterberger, W.; Gabasch, H.; Hayek, K.; Klötzer, B. *Catal. Lett.* **2005**, *104*, 1.
(16) Kaltchev, M.; Thompson, A. W.; Tysoe, W. T. *Surf. Sci.* **1997**, *391*, 145.
(17) Kesmodel, L. L.; Gates, J. A. *Surf. Sci.* **1981**, *111*, L747.
(18) Sock, M.; Eichler, A.; Surnev, S.; Anderson, J. N.; Klötzer, B.; Hayek, K.; Ramsey, M. G.; Netzer, F. P. *Surf. Sci.* **2003**, *545*, 122.
(19) Gates, J. A.; Kesmodel, L. L. *Surf. Sci.* **1983**, *124*, 68.
(20) Kesmodel, L. L. *J. Electron Spectrosc. Relat. Phenom.* **1983**, *29*, 307.
(21) Jungwirthova, I.; Kesmodel, L. L. *J. Phys. Chem. B* **2001**, *105*, 674.
(22) Ziemecki, S. B.; Jones, G. A.; Swartzfager, D. G.; Harlow, R. L.; Faber, J., Jr. *J. Am. Chem. Soc.* **1985**, *107*, 4547.
(23) Siller, R. H.; Oates, W. A.; McLellan, R. B. *J. Less-Common Met.* **1968**, *16*, 71.
(24) Paál, Z.; Wild, U.; Schlögl, R. *Phys. Chem. Chem. Phys.* **2001**, *3*, 4644.
(25) Bowker, M.; Morgan, C.; Couves, J. *Surf. Sci.* **2004**, *555*, 145.
(26) Bowker, M.; Morgan, C.; Perkins, N.; Holroyd, R.; Fourre, E.; Grillo, F.; MacDowall, A. *J. Phys. Chem.* **2005**, *109*, 2377.
(27) Shaikhutdinov, S. K.; Frank, M.; Bäumer, M.; Jackson, S.; Oldman, R. J.; Hemminger, J. C.; Freund, H.-J. *Catal. Lett.* **2002**, *80*, 115.
(28) Bertarione, J. S.; Scarano, D.; Zecchina, A.; Johanek, V.; Hoffmann, J.; Schauermann, S.; Libuda, J.; Rupprechter, G.; Freund, H.-J. *J. Catal.* **2004**, *223*, 64.
(29) Morkel, M.; Kaichev, V. V.; Rupprechter, G.; Freund, H.-J.; Prosvirin, I. P.; Bukhtiyarov, V. I. *J. Phys. Chem. B* **2004**, *108*, 12955.
(30) Borasio, M.; Rodriguez de la Fuente, O.; Rupprechter, G.; Freund, H.-J. *J. Phys. Chem. B* **2005**, *109*, 17791.
(31) Bozack, M. J.; Muehlhoff, L.; Russell, J. N., Jr.; Choyke, W. J.; Yates, J. T., Jr. *J. Vac. Sci. Technol., A* **1987**, *5*, 1.
(32) King, D.; Wells, M. G. *Surf. Sci.* **1972**, *29*, 454.
(33) Sjövall, P.; Uvdal, P. *Chem. Phys. Lett.* **1998**, *355*, 282.
(34) Tysoe, W. T.; Nyberg, G. L.; Lambert, R. M. *J. Phys. Chem.* **1984**, *88*, 1960.
(35) Kiskinova, M.; Bliznakov, G. *Surf. Sci.* **1982**, *123*, 61.
(36) Nishijima, M.; Yoshinobu, J.; Sekitani, T.; Onchi, M. *J. Chem. Phys.* **1989**, *90*, 5114.
(37) Rose, M. K.; Borg, A.; Mitsui, T.; Ogletree, D. F.; Salmeron, M. *J. Chem. Phys.* **2001**, *115*, 10927.
(38) Yudanov, I. V.; Neyman, K. M.; Rösch, N. *Phys. Chem. Chem. Phys.* **2004**, *6*, 116.
(39) Ovesson, S.; Bogicevic, A.; Wahnström, G.; Lundqvist, B. I. *Phys. Rev. B* **2001**, *64*, 125423.
(40) Morkel, M.; Rupprechter, G.; Freund, H.-J. *Surf. Sci. Lett.* **2005**, *588*, L209.
(41) Pallassana, V.; Neurock, M.; Lusvardi, V. S.; Lerou, J. J.; Kragten, D. D.; van Santen, R. A. *J. Phys. Chem. B* **2002**, *106*, 1656.